Iranian Veterinary Surgery Association

IRANIAN JOURNAL OF VETERINARY SURGERY

Journal homepage: www.ivsajournals.com

ORIGINAL ARTICLE

Influence of *Ferula assa-foetida* Loaded Chitosan Nanoparticle Biofilm on Wound Healing in Full-Thickness Wounds Infected with Methicillin Resistant *Staphylococcus aureus*

Mohammad Ali Sadeghi[1], Shayan Kalantari[1], Fatemeh Zahra Gharib[1], Firouz Faed-Maleki[2]*, Alireza Yousefi[1]

[1] *Department of Veterinary Clinical Sciences, Faculty of Veterinary Medicine, Babol Branch, Islamic Azad University, Babol, Iran.*

[2] *Department of Pharmacology, Faculty of Veterinary Medicine, Babol Branch, Islamic Azad University, Babol, Iran.*

Received: 14 September 2019
Accepted: 17 December 2019
Online: 17 December 2019

Keywords:

MRSA;

Ferula assa-foetida;

Chitosan nanoparticles biofilm;

Infected wound.

Abstract

Objective- Cutaneous wound healing is an essential physiological process consisting of the collaboration of many cell strains and their products. Initiation of new management for treatment of wound infections caused by multidrug resistant *Staphylococcus aureus* is required. The aim of the present study was to assess wound healing activity of *Ferula assa-foetida* loaded chitosan nanoparticle biofilm in methicillin resistant *S. aureus* (MRSA) infected wounds in rats.

Design- Experimental study

Animals- Forty eight male healthy Wistar rats.

Procedures- The animals were randomized into four groups of 12 animals each. In group I, the wounds were infected with MRSA and only treated with 0.1 mL the sterile saline 0.9% solution. In group II, the infected wounds were dressed with chitosan nanoparticles biofilm. In group III, animals with infected wounds were treated with 0.1 mL topical application of *Ferula assa-foetida*. In group IV, animals with infected wounds were dressed with *Ferula assa-foetida* loaded chitosan nanoparticles biofilm.

Results- Microbiological examination, planimetric, biomechanical, histological and quantitative morphometric studies and determination of hydroxyproline levels showed that there was significant difference between animals in group IV compared to other groups (p = 0.001).

Conclusion and Clinical Relevance- *Ferula assa-foetida* loaded chitosan nanoparticles biofilm could be useful for treatment of MRSA infected wounds in diabetes.

* Correspondence to: Firouz Faed-Maleki, Department of pharmacology, Babol Branch, Islamic Azad University, Babol, Iran. E-mail: faedmalekif@yahoo.com

DOI: 10.22034/ivsa/ivsa.2019.201547.1200

1. Introduction

Cutaneous wound healing is an essential physiological process consisting of the collaboration of many cell strains and their products.[1] Attempts to restore the lesion induced by a local aggression begin very early on in the inflammatory stage. In the end, they result in repair, which consists of the substitution of specialized structures brought about by the deposition of collagen, and regeneration, which corresponds to the process of cell proliferation and posterior differentiation through preexisting cells in the tissue and/or stem cells.[2] These mechanisms do not mutually exclude themselves, that is, after a skin lesion, in the same tissue, regeneration and repair can occur, depending on the cell strains compromised by the injury.

The oleo-gum-resin *Asafoetida* is called "Anguzakoma", "Anghouzeh", and "Khorakoma" in Iran. *Ferula assa-foetida* is the plant utilized for manufacture of dried latex (gum oleoresin) which is exuded from the rhizome and stems of this plant belonging to the family Umbelliferae. A milky secretion exudes from the cut surface of rhizome, stems and the dried exudates are scraped off. The plant grows 1-1.5 m tall and possesses extremely dissected leaves the inconspicuous yellow flowers have been kept in compound umbels. The bark is black and wrinkled which contains great amounts of gelatinous alliaceous juice.[3,4] It is used in the treatment of various diseases such as intestinal parasites, flatulence, influenza, epilepsy, stomachache, asthma, and weak digestion.[5] The pharmacological studies have demonstrated its antioxidant, antifungal and antimicrobial properties.[6-9]

Chitosan is a b-1,4-linked polymer of glucosamine (2-amino-2-deoxy-b-d-glucose) and lesser amounts of N-acetylglucosamine. It is a derivative of chitin (poly-N-acetylglucosamine) which is the second most abundant biopolymer after cellulose. Chitosan was first discovered in 1811 by a French chemist and pharmacist.[10] Chitosan, as a cationic natural polymer, has been widely investigated as an antimicrobial agent for preventing and treating infections due to its intrinsic antimicrobial properties, and also its ability to effectively deliver extrinsic antimicrobial compounds into the infected area.[10]

It has been proposed that interaction between positively charged chitosan molecules and negatively charged microbial cell membranes leads to the disruption of microbial membrane and subsequently the leakage of proteinaceous and other intracellular constituents.[11-14] One factor that limits the application of native chitosan is its non-solubility in neutral and alkaline aqueous solutions. In vitro studies have demonstrated the significant biofilm efficacy of chitosan nanoparticles.[15,16]

To the best knowledge of the authors the literature is poor regarding potentiation effects of *Ferula assa-foetida* in combination with chitosan nanoparticle biofilm on wound healing in full thickness infected wounds with antibiotic resistant gram positive bacteria. Therefore, the present study aimed to study effects of propoplis loaded chitosan nanoparticle biofilm on wound healing in full thickness infected wounds with methicillin resistant *Staphylococcus aureus* (MRSA). The assessments were based on excision wound model and planimetric studies, histological preparation and quantitative morphometric studies and determination of hydroxyproline levels.

2. Materials and Methods

All antibiotics and reagents were research grade and purchased from Sigma-Aldrich, St. Louis, MO. and used without further purification. Methicillin stock was suspended in water. The Antibiotic stock was diluted at least 100-fold in phosphate buffered saline (PBS), pH 7.4, before use in the assays. The study was approved by the institutional animal research ethics committee and 3R's principles (Replacement, Reduction and Refinement) were strictly followed. Forty eight adult healthy male Wistar rats weighting 200– 250 g were used and housed in individual cages under constant temperature (22º C) and humidity

with natural light/dark cycle, and had *ad libitum* access to chow and water throughout the study.

Preparation of MP (Carrier)

To prepare 100 g of Macrogol ointment, 40 g of polyethylene glycol 3350 (Ineos Manufacturing, Deutschland GmbH, Germany) was mixed with 60 g of polyethylene glycol 400 (DOW Chemical Company, USA). The two ingredients were heated in water bath at 65° C until complete melting and then allowed to cool down to room temperature while stirring until the mixture was congealed.

Formation of the Ferula assa-foetida Paste

To prepare 50 g of *Ferula assa-foetida* paste, 15 g of *Ferula assa-foetida* was mixed well with 35 g of MP in a sterile mortar to obtain a creamy paste.

Preparation of Chitosan Nanoparticle Biofilm

The chitosan nanoparticles were prepared based on a procedure described by others.[17] A 2.5 mg/ml chitosan solution was prepared by dissolving LMW or VLMW chitosan in a 0.05% (v/v) acetic acid solution and leaving it under stirring for 24 h. The pH was adjusted to 5.5with a 0.5 M sodium hydroxide solution and diluted in deionized water to the final desired concentrations. The tripolyphosphate (TPP) was dissolved in deionized water to a final concentration of 0.25 mg/ml. TPP and chitosan solutions were filtered through a 0.45 µm membrane (Millipore). Then, the TPP solution was added to the chitosan solution drop wise (0.3 mL/min) at different TPP: chitosan ratios under vigorous magnetic stirring at room temperature. The resulting suspension was dissolved in 100 mL of 1% acetic acid and stirred for 24 h at room temperature. The obtained solution was then filtered through G4 sand filter in order to remove the impurities and undissolved particles. The prepared plain polysulfone (PSf/TiO2) membrane (100 cm^2) was pasted on the glass plate separately using tape with thickness of 1 mm. The stuck membrane was washed with distilled water and wiped with smooth tissue paper. A thin film of saturated polyvinyl alcohol solution was brush coated on the substrate. Chitosan (30 ml) was slowly poured in the center of the substrate and spread evenly throughout the substrate. Further, the thin film was dried at 60° C for 4 h in a hot air oven. After drying, the membrane was allowed to reach room temperature, and was then washed with 1% NaOH to remove excess acetic acid. Finally, the membrane was washed with distilled water until the washed water reached neutral ph. The same was repeated for bare PSf membranes.[18] The obtained membranes were used to dress the wounds. Scanning electron microscopy (SEM) imaging was used to determine structural characterization of the biofilm (Figure 1).

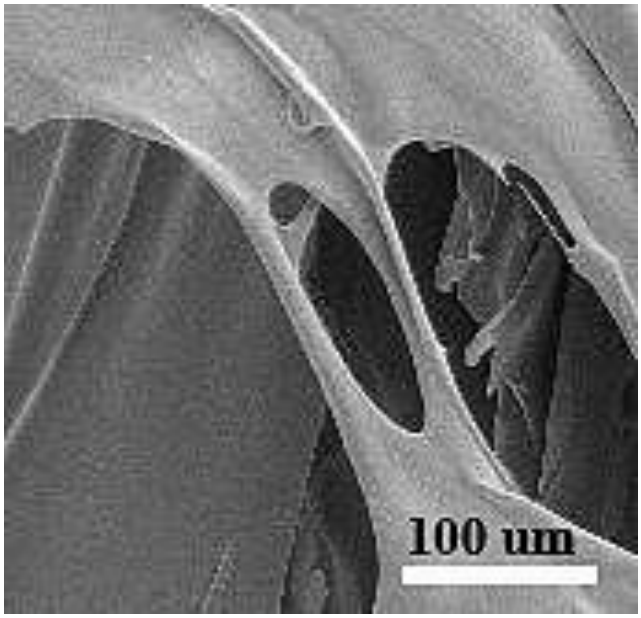

Figure 1. Scanning electron microscopy (SEM) micrograph of chitosan nanoparticles biofilm.

Wound Creation and Infection

Rats were anesthetized by an intraperitoneal injection of ketamine (70 mg/kg of BW) and xylazine (5 mg/kg of BW), the hair on their back was shaved and the skin cleansed with 70% alcohol solution. Following shaving

and aseptic preparation, a circular excision wound was made by cutting away approximately 115 mm^2 full thickness of predetermined area on the anterior-dorsal side of each rat. Small gauze was placed over each wound and then inoculated with 5×10^7 CFU of *Staphylococcus aureus* ATCC 43300. The methicillin-resistant *S. aureus* ATCC 43300 strain was commercially available. The pocket was closed by means of 4-0 nylon sutures and this procedure resulted in a local abscess after 24 h. The rats were returned to individual cages and they were examined daily. After 24 h, the wounds were opened, the gauze removed for quantitative bacterial cultures and treatment started.

Study Design and Animals

This study was carried out in strict accordance with the guidelines of the Ethics Committee of the International Association for the Study of Pain.[19] All bacterial inoculations and treatments were performed under conditions to minimize any potential suffering of the animals. Forty eight male rats were randomized into four groups of 12 animals each. In group I, the wounds were infected with MRSA and only treated with 0.1 mL the sterile saline 0.9% solution. In group II, the infected wounds were dressed with chitosan nanoparticles biofilm. In group III, animals with infected wounds were treated with 0.1 ml topical application of *Ferula assa-foetida*. In group IV, animals with infected wounds were dressed with *Ferula assa-foetida* loaded chitosan nanoparticles biofilm. All the test formulations were applied for 10 days, twice a day, starting from the first treatment.

Microbiological Assessments

Briefly, for total bacterial count on days 2, 4 and 6 of treatment after wound creation the granulated tissues were excised aseptically. Then, 0.1 g of sample was crushed and homogenized in sterile mortar containing 10 ml of sterile saline. The homogenized sample was serially diluted in tube containing 9 ml of sterile saline to 10-5. The diluted samples were cultured on plate count agar (Merck KGaA, Darmstadt, Germany) superficially and duplicated. The cultured plates were incubated at 37º C for 24 to 48 hours. After incubation, all colonies were counted and results described as CFU/g of granulation tissue.[20]

Excision Wound Model and Wound Area Measurements

Wound-healing property was evaluated by wound contraction percentage and wound closure time. Photographs were taken immediately after wounding and on days 6, 9, 12, 15, 18, and 21 post-wounding by a digital camera while a ruler was placed near the wounds. The wound areas were analyzed by Measuring Tool of Adobe Acrobat 9 Pro Extended software (Adobe Systems Inc, San Jose, CA, USA) and wound contraction percentage was calculated using the following formula:

Percentage of wound contraction = $(A_0 – A_t) / A_0 \times 100$

Where A_0 is the original wound area and A_t is the wound area at the time of imaging. Animal houses were in standard environmental conditions of temperature (22 ± 3° C), humidity (60 ± 5%), and a 12 h light/dark cycle. The animals were maintained on standard pellet diet and tap water. All rats were closely observed for any infection and if they showed signs of infection were separated, excluded from the study and replaced.

Incision Wound Model and Biomechanical Testing

Twenty-four healthy male Wistar rats weighing 160-180 g approximately seven weeks of age were randomized into four groups of 6 rats each as described for excisional wound model. All animals of four groups were anesthetized as mentioned above and a paravertebral long incision of 4 cm length was made through the skin and cutaneous muscle at a distance about 1.5 cm from the middle on right side of the depilated back. After the incision was made, the two ends of the wound were

sutured at 0.5 cm intervals with 3-0 nylon. The formulations were applied the same way in the excisional wound model. On day 9, sutures were removed and a strip of skin, 7 cm long, with the same widths of wound diameter, in the manner that the wound was located at the middle of the strip, was removed by a double-blade scalpel. The skin was then wrapped in Ringer's soaked gauze, aluminum foils, and plastic bags and kept in −20° C freezer until mechanical testing. The TA.XTPlus Texture Analyzer mechanical test device was used for the assessment (Stable Micro Systems, Surrey GU7 1YL, UK). The samples were fitted with appropriate clamps, the distance between the clamps at the start of testing being 4 cm. The strips were loaded with 0–30 kg load cell, with strain rate of 1 cm/min and the load elongation curves were obtained. Yield strength (yield point) (kg), ultimate strength (kg), maximum stored energy (kg/cm), and stiffness (kg/cm) were measured from the load elongation curves.

Histology and Morphometric Studies

The tissue samples were taken on 7, 14, and 21 days after surgery from periphery of the wound along with normal skin and fixed in 10% buffered formalin, dehydrated and embedded in paraffin wax, sectioned at 5 µm and stained with hematoxylin and eosin (H&E) and Masson's trichrome stains. Photomicrographs were obtained under light microscope to assess the predominant stage of wound healing. Three parallel sections were obtained from each specimen. Cellular infiltration including the number of mononuclear cells, polymorphonuclear cells and fibroblastic aggregation were quantitatively evaluated. Acute hemorrhage, congestion, vascularization, epithelialization, collagen production and density were also evaluated qualitatively. Morphological findings were scored using image analyzing software (Image-Pro Express, version 6.0.0.319, Media Cybernetics, Silver Springs, MD, USA). The histological parameters were classified according to the intensity of occurrence in five levels (- absence; + discrete; ++ moderate; +++ intense; ++++ very intense).[21]

Determination of Hydroxyproline Levels

On the day 21 after surgery, a piece of skin from the healed wound area was collected and analyzed for hydroxyproline content. As a major part of collagen, hydroxyproline has an essential role in collagen stability. The collagen is the major component of extracellular tissue, which gives support and strength. Tissues were dried in a hot air oven at 60–70° C to constant weight and were hydrolyzed in 6N HCl at 130° C for 4 h in sealed tubes. The hydrolysate was neutralized to pH 7.0 and was subjected to chloramine-T oxidation for 20 min. The reaction was terminated by addition of 0.4M perchloric acid and color was developed with the help of Ehrlich reagent at 60° C and measured at 557 nm using UV-visible spectrophotometer.

Statistical Analyses

Differences among groups were evaluated by Kruskal–Wallis variance analysis. When the *p*-value from the Kruskal–Wallis test statistics was statistically significant, multiple comparison tests were used to know differences. Comparison among days was assessed by Mann–Whitney U-test. The Bonferroni correction was applied for all possible multiple comparisons. SPSS 18 (SPSS Inc., Chicago, IL, USA) was used for statistical analysis. A *p*-value was set at 0·05.

3. Results

Microbiological Assessments

In animals of group V whose infected wounds were treated with *Ferula assa-foetida* loaded chitosan nanoparticles biofilm, the counts of *S. aureus* cultured in the wound tissues were significantly lower than in the infected wounds in other groups ($p = 0.001$). No animals died due to infection or anesthetics. The uninfected wounds treated

with saline had no CFU/g of *S. aureus* count. Dressing of the wounds with *Ferula assa-foetida* loaded chitosan nanoparticles biofilm significantly reduced the rate of total bacterial count post-wounding compared to other groups (p = 0.001) (Table 1).

Table 1. Wound bacterial count (CFU/g) of granulation tissue in experimental groups on three time points of 2, 4, and 6 days. Data are expressed as Mean ± SD.

	2nd day	4th day	6th day
Group I	2153.14 ± 116.25	1456.51 ± 165.13	994.54 ± 96.73
Group II	1156.70 ± 61.10	915.19 ± 28.45	310.78 ± 24.15*
Group III	1502.60 ± 77.60	1008.84 ± 31.24	682.65 ± 37.64
Group IV	514.20 ± 45.59*	284.70 ± 44.12*	154.79 ± 31.19*

CFU: Colony-forming units. *p < 0.05 *vs.* groups II and III.

Reduction in Wound Area

Wound contraction percentage in different groups within the study period is shown in Figure 1. The healing rate of wounds in group IV was significantly different compared to groups II and III (p = 0.001).

Biomechanical Findings

The biomechanical indices, maximum stored energy, stiffness, ultimate strength and yield strength obtained for group IV were significantly higher than those obtained for other groups (p = 0.002) (Table 2). This indicated better biomechanical properties of the dressing with *Ferula assa-foetida* loaded chitosan nanoparticle biofilm on treated tissues.

Histological and Morphometric Findings

There were significant differences in comparisons of groups IV and III, particularly in terms of cellular infiltration, acute hemorrhage, congestion, edema, collagen production and density, reepithelialization and neovascularization. During the study period, scores for reepithelialization and neovascularization were significantly higher in group IV rats than groups II and III (p = 0.001). Polymorphonuclear (PMN) and mononuclear (MNC) cell count, fibroblast cell proliferation and also Mean Rank of the qualitative study of acute hemorrhage, edema and collagen production scores in group IV were significantly higher than those of groups II and III (p =0.001) (Figures 2-7).

Hydroxyproline Content of Wound

Proline is hydroxylated to form hydroxyproline after protein synthesis. Hydroxyproline contents in groups I to IV were found to be 41.58 ± 2.54, 61.37 ± 3.26, 69.65 ± 3.24, and 96.43 ± 3.16 mg/g, respectively. Hydroxyproline contents were significantly increased in the group IV which implies more collagen deposition compared to groups II and III (p = 0.001).

Table 2. Biomechanical parameters of the experimental groups. Data are expressed as Mean ± SD.

group	Ultimate strength (kg/cm)	Stiffness (kg/cm)	Maximum stored energy (Kg)	Yield point
I	0.67 ± 0.10	0.72 ± 0.17	0.40 ± 0.15	**0.63 ± 0.12**
II	1.01 ± 0.12	0.81 ± 0.11	0.48 ± 0.18	**1.43 ± 0.14**
III	0.76 ± 0.12	0.95 ± 0.14	0.95 ± 0.18	**1.13 ± 0.22**
IV	1.95 ± 0.16*	2.01 ± 0.12*	2.11 ± 0.15*	**2.32 ± 0.21***

The treated groups are compared by Student t-test with other groups. *: The mean difference was significant at the .05 level *vs.* groups II and III.

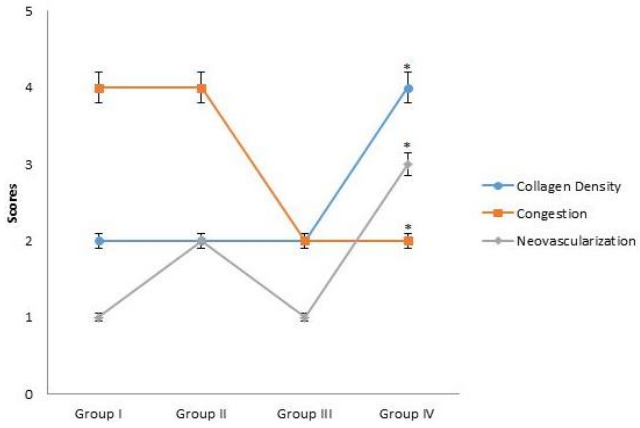

Figure 2. Line Graph indicating evaluation of Intensity of histological parameters in experimental groups. Results were expressed Mean ± SEM. *p < 0.05 vs other experimental groups.

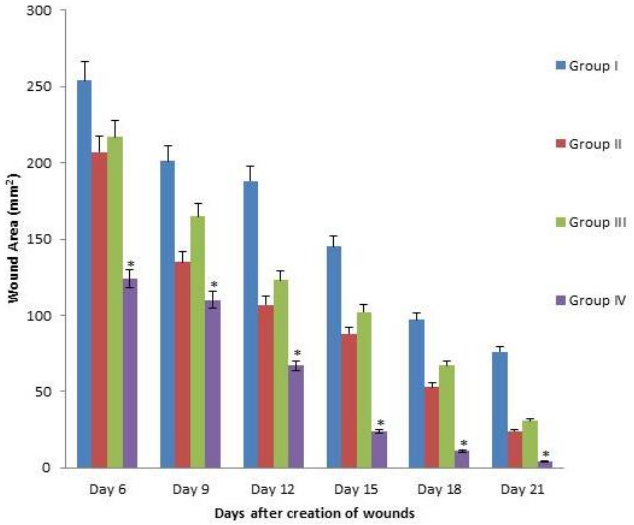

Figure 3. Bar Graph showing area of wounds in excisional model of the rats' skin in experimental groups. Results were expressed as mean ± SEM. * $p < 0.05$ vs other experimental groups.

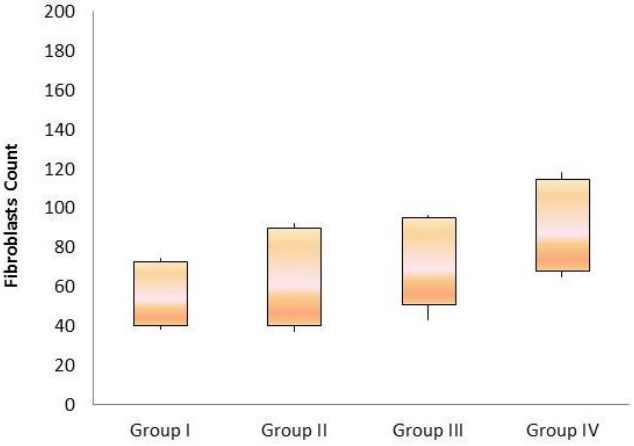

Figure 4. Box-whisker plot indicating number of fibroblasts in excisional model of the rats' skin in experimental groups.

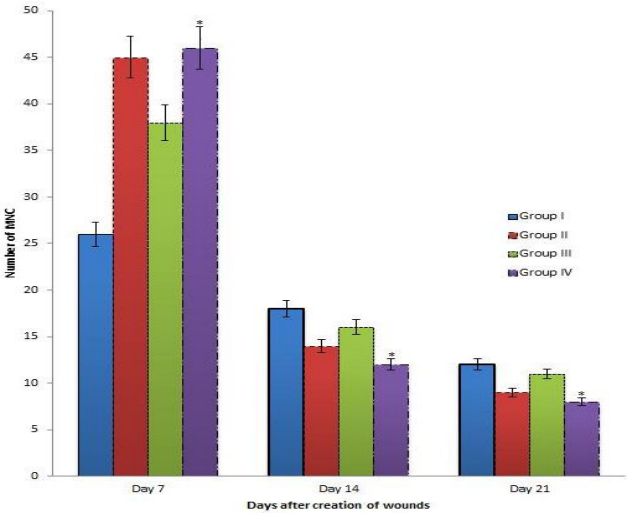

Figure 5. Box-whisker plot indicating number of PMN cells in excisional model of the rats' skin in experimental groups.

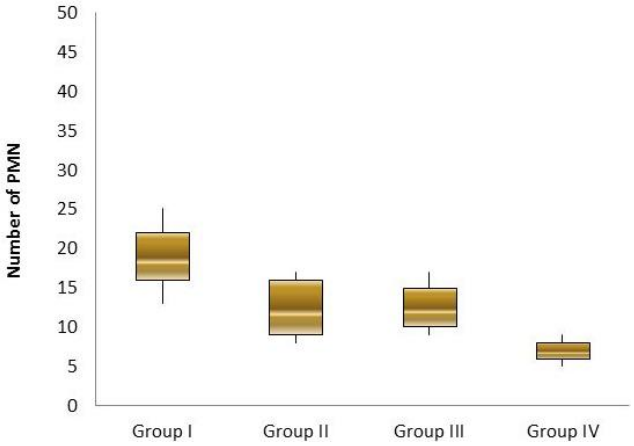

Figure 6. Bar graph indicating number of mononuclear cells (MNC) in excisional model of the rats skin in experimental groups. Results were expressed as mean ± SEM. *$p < 0.05$ vs other experimental groups.

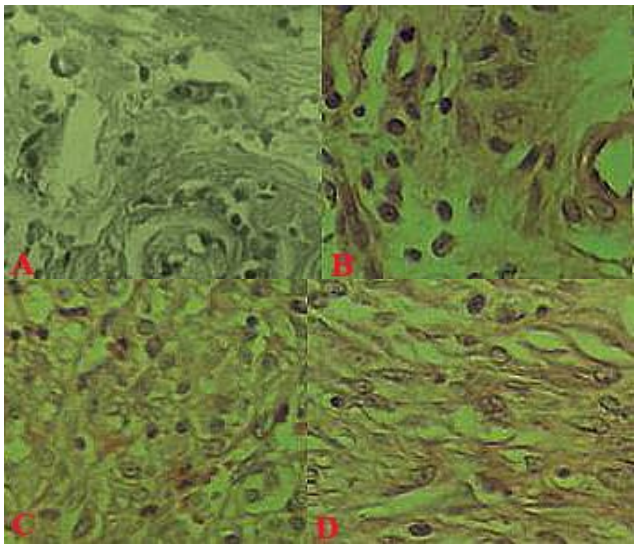

Figure 7. Histological characteristics of rat skin on day 14 after wound creation in excisional wound model. A: Group I, B: Group II, C: Group III and D: Group IV. Wounds with surrounding skin were prepared for histological microscopic evaluation by H&E staining (400×).

4. Discussion

Wound healing is characterized by reepithelialization, granulation tissue growth and remodeling of extracellular matrix. Although the wound healing process occurs by itself, spontaneously, and does not require much help, there are various risk factors such as infection, supply of blood, nutritional status and other factors that influence the resolution of this process.[22] It is well known that attack by microbes, which invade the skin barrier, delays the natural

wound healing process.[23] MRSA is increasing in infections and is a serious threat to patients in health care facilities and the community. There are many reports in the literature that researchers have been working on various agents to combat MRSA related infections.[24-28] Resistance to common antibiotics makes treating MRSA costly and difficult. The main end point observed in this study, wound contraction and reduction in wound area, was accelerated by treating the wounds dressed with *Ferula assa-foetida* loaded chitosan nanoparticles biofilm. All the parameters observed (presence of necrotic tissue, clotting and crust, re-epithelialization and granulation tissue growth, bacterial count) were affected; suggesting that *Ferula assa-foetida* loaded chitosan nanoparticles biofilm was effective against MRSA.

In excisional wound model there was a significant decrease in wound area. This indicated improved collagen maturation by increased cross linking. The balance between synthesis and breakdown and so deposition of collagen is important in wound healing and development of wound strength .[29] Hydroxyproline is a major component of the collagen that permits the sharp twisting of the collagen helix. It helps on providing stability to the triple-helical structure of collagen by forming hydrogen bonds. Hydroxyproline is found in few proteins other than collagen. For this reason, hydroxyproline content has been used as an indicator to determine collagen content.[30] Increase in hydroxyproline content in group IV indicated increased collagen content, since hydroxyproline is the direct estimate of collagen synthesis.

Increase in hydroxyproline content in group IV indicated increased collagen. Mechanical testing is sensitive to changes that occur during the progression of wound healing, and can be used as a tool to measure the quality of healing. Mechanical property data provide a clinically relevant and functional assessment of wound healing quality. In the present study the depressing of the wounds with *Ferula assa-foetida* loaded chitosan nanoparticles biofilm improved mechanical properties of the tissue, hence, the integrity of the repaired tissue was retrieved.

Our preliminary data showed that *Ferula assa-foetida* loaded chitosan nanoparticles biofilm significantly reduced tissue bacteria count and promoted the healing stages. Accordingly, the animals in group IV showed shortened homeostasis and inflammatory phases and accelerated proliferation and maturation stages. Considering the importance of the bacterial infection as well as presence of pathogens in wound tissue, we analyzed the MRSA colonies count in wound area. The observations demonstrated that the infection was controlled after dressing with *Ferula assa-foetida* loaded chitosan nanoparticles biofilm The inflammation phase is considered as a main step in order to eliminate cellular debris from tissue as well as extensive response for microbial infection.[31,32] Therefore, rapid inflammatory response is necessary to control the inflammation. Neutrophils, macrophages and lymphocytes infiltrate to the site of injury during inflammatory stage.[31,32] Light microscopic analyses showed that in group IV mononuclear immune cell infiltration was significantly increased on day 8 post operation. This situation plays a critical role in eliminating the infection and provoking the healing process by considering the key role of inflammatory cells (especially macrophages) in organizing the granulation tissue. Therefore, the antibacterial impact of *Ferula assa-foetida* loaded chitosan nanoparticles biofilm may largely correlates with these agents.

The observations of our study showed that *Ferula assa-foetida* loaded chitosan nanoparticles biofilm resulted in enhanced cellular proliferation. The fibroblasts and fibrocytes distribution in one mm^2 of the wound site was significantly higher in comparison with other groups. Regarding the key role of fibroblasts and fibrocytes in synthesis of collagen, we could hypothesize that elevated collagen deposition in group IV was attributed to high cellularity of fibroblasts and fibrocytes. Increased neovascularization on day 8 following wound induction showed *Ferula assa-foetida* loaded chitosan nanoparticles

biofilm could provoke the healing process via stimulating cells infiltration after 8 days.

The key point to end of the inflammation is the apoptotic activity of immune cells. Apoptosis is considered a vital component of various processes including normal cell turnover, proper development and functioning of the immune system, hormone-dependent atrophy, embryonic development, and chemical-induced cell death.[33] In the inflammation response, the mediators induce the infiltration of activated immune cells into inflammation site to protect the tissue against the pathogen infection. In the end of the inflammation, apoptosis of the immune cells and the apoptotic cells are cleared by macrophages. The clearance by macrophages of cells apoptosis is a key point phenomenon associated with actively tissue formation from wound inflammation.[34-36]

With respect to wound-healing effects, it has been indicated from in vitro studies that chitosan enhances the functions of PMN, macrophages and fibroblasts. As a result, chitosan promotes granulation and organization. Most of the animal and clinical studies reported that chitosan preparations accelerate the wound healing. The infiltration of PMN cells and production of fibroblasts are promoted. The number of inflammatory cells in the wound is reduced. In addition, chitosans are nontoxic to normal cells. However, side effects of some chitosan preparations were also reported and chitosan was also found to be ineffective in corneal wound healing.[37-39] With respect to the physical and biological properties, it was concluded from the studies in this review that chitosan, as a wound dressing, must be rapidly and uniformly adherent and conform to wound bed topography and contours to prevent air or fluid pocket formation. The dressing is preferably permeable to water vapor so that a moist exudate under the dressing is maintained without pooling. The large number of publications in this area suggests that chitosan will continue to be an important agent in the management of wounds and burns. The free radicals play a key role in various disease conditions. The biochemical reactions generate reactive oxygen species in our body which are capable of damaging essential bio-molecules. If, reactive oxygen species are not effectively scavenged by cellular constituents, they cause disease conditions.[40] Such actions of free radicals can be blocked by antioxidant substances by scavenging them and detoxify the organism.

Antioxidants have been reported to play a significant role in improving the wound-healing process and protecting the tissues from oxidative damage.[41] Wound-healing mechanisms may be contributed to stimulate the production of antioxidants in wound site and to provide a favourable environment for tissue healing.[42] It has been recently published that *Ferula assa-foetida* has essential oil components.[43] The antioxidant activity of the essential oil components from the *Ferula assa-foetida* was examined by *in vitro* 1,1-Diphenyl-2- picryl-hydrazyl (DPPH) and nitric oxide radical scavenging assay, reducing power, linoleic acid and iron ion chelation power and it was established that it bears antioxidant activity. The extract from aerial parts of *Ferula assa-foetida* showed various levels of antioxidant activity in all the models studied. These extracts had good Fe++ chelation ability; DPPH and nitric oxide radicals scavenging activities.[6]

In conclusion, our results showed that *Ferula assa-foetida* loaded chitosan nanoparticles biofilm was useful for treatment of MRSA infected wounds and had the potential to offer a return to this safer agent for topical use. Dose-response studies are needed to study various concentrations for *Ferula assa-foetida* and chitosan nanoparticles biofilm for determination of optimum dosages to achieve maximum effects.

Acknowledgments

We would like to thank the deputy for Research of the Islamic Azad University, Babol Branch, for their kind cooperation.

Conflicts of Interest

None.

References

1. Shaw TJ, Martin P. Wound repair at a glance. *Journal of Cell Science*. 2009; 122: 3209-3213.
2. Eming SA, Krieg T, Davidson JM. Inflammation in wound repair: molecular and cellular mechanisms. *Journal of Investigative Dermatology*. 2007; 127: 514-525.
3. Behpour M, Ghoreishi S, Khayatkashani M, Soltani N. The effect of two oleo-gum resin exudate from *Ferula assa-foetida* and *Dorema ammoniacum* on mild steel corrosion in acidic media. *Corrosion Science*, 2011; 53: 2489-2501.
4. Golmohammadi F. Medical plant of Ferula assa-foetida and its cultivating, main characteristics and economical importance in south Khorasan province-east of Iran. *Journal of Applied Science, Engineering* and *Technology*, 2013; 3: 2334-2346.
5. Lee CL, Chiang LC, Cheng LH, Liaw CC, Abd El-Razek MH, Chang FR, Wu YC. Influenza A (H1N1) antiviral and cytotoxic agents from *Ferula assa-foetida*. *Journal of Natural Products*, 2009; 72(9): 1568-1572.
6. Dehpour AA, Ebrahimzadeh MA, Fazel NS, Mohammad NS. Antioxidant activity of the methanol extract of *Ferula assa-foetida* and its essential oil composition. *Grasas Y Aceites*, 2009; 60: 405-412.
7. Angelini P, Pagiotti R, Venanzoni R, Granetti B. Antifungal and allelopathic effects of asafoetida against *Trichoderma harzianum* and Pleurotus spp. *Allelopathy Journal*, 2009; 23: 357-368.
8. Sitara U, Niaz I, Naseem J, Sultana N. Antifungal effect of essential oils on in vitro growth of pathogenic fungi. *Pakistan Journal of Botany*, 2008; 40: 409-144.
9. Singh R. In vitro evaluation of aqueous and alcoholic extracts of spices for antifungal properties. *Indian Journal of Animal Sciences*, 2007; 77: 675-677.
10. Tang H, Zhang P, Kieft TL, Ryan SJ, Baker SM, Wiesmann WP, Rogelj S. Antibacterial action of a novel functionalized chitosan-arginine against Gram-negative bacteria. *Acta Biomaterialia*, 2010; 6(7): 2562–2571.
11. Li P, Poon YF, Li W, Yeap SH, Cao Y, Qi X, Zhou C, Lamrani M, Beuerman RW, Kang ET, Mu Y, Li CM, Chang MW, Leong SS, Chan-Park MB. A polycationic antimicrobial and biocompatible hydrogel with microbe membrane suctioning ability. *Nature Materials*, 2011; 10(2): 149–156.
12. Kong M, Chen XG, Xing K, Park HJ. Antimicrobial properties of chitosan and mode of action: a state of the art review. *International Journal of Food Microbiology*, 2010; 144(1): 51–63.
13. Andres Y, Giraud L, Gerente C, Le Cloirec P. Antibacterial effects of chitosan powder: mechanisms of action. *Environmental Technology*, 2007; 28(12): 1357–1363.
14. Raafat D, von Bargen K, Haas A, Sahl HG. Insights into the mode of action of chitosan as an antibacterial compound. *Environmental Microbiology*, 2008; 74(12), 3764–3773.
15. Silva PV, Guedes DF, Nakadi FV, Pecora JD, Cruz-Filho AM. Chitosan: a new solution for removal of smear layer after root canal instrumentation. *International Endodontic Journal*, 2013; 46: 332-338.
16. Calamari SE, Bojanich MA, Barembaum SR, Berdicevski N, Azcurra AI. Antifungal and post-antifungal effects of chlorhexidine, fluconazole, chitosan and its combinations on *Candida albicans*. *Medicina Oral Patologia Oral y Cirugia Bucal*, 2011; 16: 23-28
17. Rampinoa A, Borgognaa M, Blasi P, Bellicha B, Cesàro A. Chitosan nanoparticles: Preparation, size evolution and stability. *International Journal of Pharmaceutics*, 2013; 455(1-2): 219-228.
18. Nayak V, Jyothi MS, Balakrishna RG, Padaki M, Ismail AF. Preparation and characterization of chitosan thin films on mixed-matrix membranes for complete removal of chromium. *Chemistry Open* 2015; 4(3): 278–287.
19. Zimmermann M. Ethical guidelines for investigations of experimental pain in conscious animals. *Pain*, 1983; 16: 109-110.
20. Kumar MS, Kirubanandan, S, Sripriya R, Sehgal PK. Triphala promotes healing of infected full-thickness dermal wound. *Journal of Surgical Research*, 2008; 44(1): 94-101.
21. Qiu Z, Kwon AH, Kamiyama Y. Effects of plasma fibronectin on the healing of full-thickness skin wounds in streptozotocin-induced diabetic rats. *Journal of Surgical Research*, 2007; 138(1): 64-70.
22. Peters EJ, Lipsky BA. Diagnosis and management of infection in the diabetic foot. *Medical Clinics of North America*, 2013; 97(5): 911-946
23. Pattanayak SP, Sunita P. Wound healing, anti-microbial and antioxidant potential of *Dendrophthoe falcata* (L.f) Ettingsh. *Journal of Ethnopharmacology*. 2008; 120(2): 241-247.
24. Jonaidi J, Kargozari N, Ranjbar M, Rostami RH,

Hamedi H. The effect of chitosan coating incorporated with ethanolic extract of propolis on the quality of refrigerated chicken fillet. *Journal of Food Processing and Preservation*, 2018; 11: 1-8.
25. Maghsoudi O, Ranjbar R, Mirjalili SH, Fasihi-Ramandi M. Inhibitory activities of platelet-rich and platelet-poor plasma on the growth of pathogenic bacteria. *Iranian Journal of Pathology.* 2017; 12(1): 79-87.
26. Ranjbar R, Shahreza MHS, Rahimi E, Jonaidi-Jafari N. Methicillin-resistant staphylococcus aureus isolates from iranian restaurant food samples: Panton-valentine leukocidin, sccmec phenotypes and antimicrobial resistance. *Tropical Journal of Pharmaceutical Research*, 2017; 16(8): 1939-1949.
27. Memariani H, Shahbazzadeh D, Ranjbar R, Behdani M, Memariani M, Pooshang Bagheri K. Design and characterization of short hybrid antimicrobial peptides from pEM-2, mastoparan VT1, and mastoparan-B. *Chemical Biology Drug Design*, 2017; 89(3): 327-338.
28. Javanmardi S, Divband B. Beneficial effects of Ag-exchanged zeolite nanocomposite on excisional wound in rats. *Iranian Journal of Veterinary Surgery*, 2017; 12(1): 25-32.
29. Kazemi-Darabadi S, Akbari G, Jarolmasjed SH, Shahbazfar AA. A Histopathologic study of effects of olive oil plus lime water on third-degree burn in mouse model. *Iranian Journal of Veterinary Surgery*, 2017; 12(1): 55-63.
30. Martin J, Zenilman M, Lazarus GS. Molecular microbiology: new dimensions for cutaneous biology and wound healing. *Journal of Investigative Dermatology*, 2010; 130(1): 38-48.
31. Berridge MJ. Cell Stress, Inflammatory Responses and Cell Death. *Cell Signaling Biology*, 2014; 14(1): 1-30.
32. Boyce ST, Lalley AL. Tissue engineering of skin and regenerative medicine for wound care. *Burns Trauma*, 2018; 6: 4.
33. Elmore S. Apoptosis: a review of programmed cell death. *Toxicologic Pathology*, 2007; 35(4): 495-516.
34. Wu YS, Chen SN. Apoptotic cell: linkage of inflammation and wound healing. *Frontiers in Pharmacology*, 2014; 5: 1.
35. Rostami H, Mohammadi R, Asri-Rezaei S, Tehrani AA. Evaluation of application of chitosan/nano sodium selenite biodegradable film on full thickness excisional wound healing in rats. *Iranian Journal of Veterinary Surgery*, 2018; 13(1): 15-24
36. Shabrandi A, Azizi S, Hobbenaghi R, Ownagh A, Keshipour S. The healing effect of chitosan supported nano-CeO2 on experimental excisional wound infected with pseudomonas aeruginosa in rat. *Iranian Journal of Veterinary Surgery*, 2017; 12(2): 9-20
37. Ong SY, Wu J, Moochhala SM, Tan MH, Lu J. Development of a chitosan-based wound dressing with improved hemostatic and antimicrobial properties. *Biomaterials*, 2008; 29(32): 4323–4332.
38. Wiegand C, Winter D, Hipler UC. Molecular-weight-dependent toxic effects of chitosans on the human keratinocyte cell line HaCaT. *Skin Pharmacology and Physiology*, 2010; 23(3): 164–170.
39. Sall KN, Kreter JK, Keates RH. The effect of chitosan on corneal wound healing. *Annals of Ophthalmology*, 1987; 19(1): 31–33.
40. Halliwell B, Gutteridge JM, Cross CE. Free radicals, antioxidants and human disease: Where are we now? *Journal of Laboratory and Clinical Medicine*, 1992; 119: 598-620.
41. Galeano M, Torre V, Deodato B, Campo GM, Colonna M, Sturiale A, Squadrito F, Cavallari V, Cucinotta D, Buemi M, Altavilla D.. Raxofelast, a hydrophilic vitamin E-like antioxidant, stimulates wound healing in genetically diabetic mice. *Surgery*, 2001; 129(4): 467-677.
42. Musalmah M, Nizrana MY, Fairuz AH, NoorAini AH, Azian AL, Gapor MT, Wan Ngah WZ. Comparative effects of palm vitamin E and alpha-tocopherol on healing and wound tissue antioxidant enzyme levels in diabetic rats. *Lipids*, 2005; 40(6): 575-580.